Available online at www.sciencedirect.com

ScienceDirect

Ceramics International 38 (2012) 605–611

CERAMICS INTERNATIONAL

www.elsevier.com/locate/ceramint

Mechanical property and microstructure evolutions of C_f/SiOC composites with increasing annealing temperature in reduced pressure environment

Tianheng Xu, Qingsong Ma [*], Zhaohui Chen

National Key Laboratory of Science and Technology on Advanced Ceramic Fibers & Composites, College of Aerospace &Materials Engineering, National University of Defense Technology, Changsha 410073, PR China

Received 10 June 2011; received in revised form 24 July 2011; accepted 24 July 2011

Abstract

Three-dimensional (3D) carbon fiber reinforced silicon oxycarbide (C_f/SiOC) composites were fabricated through precursor impregnation and pyrolysis process using siloxane resin as precursor. These composites were further annealed at various temperatures to follow their mechanical properties and microstructure evolutions in reduced pressure environment. The decrease in strength of those composites could be attributed mainly to the decomposition of matrixes. When the annealing temperature increased from 1000 to 1250 °C, the mechanical properties of composites did not change too much, despite the matrixes underwent a redistribution of Si–O bonds and Si–C bonds. At temperature above 1300 °C, due to the weight loss and volume shrinkage of matrixes caused by carbothermal reduction, both the flexural strength and elastic modulus of C_f/SiOC composites decreased rapidly.

Keywords: B. Composites; C. Mechanical properties; Environmental degradation

1. Introduction

Silicon oxycarbide glasses (SiOC) can be considered as anionic modification of silica glass in which Si–O bonds are partially replaced by Si–C bonds and, thus enhance the mechanical and thermal properties of the material [1–3]. Its composition is usually reported as following equation [4]: $SiC_xO_{2(1-x)} + yC_{free}$, where $SiC_xO_{2(1-x)}$ describes the amorphous silicon oxycarbide network and C_{free} is free carbon. They are suitable materials for applications at high temperature such as fibers or matrices for ceramic matrix composites (CMCs) [5–7]. Indeed, C_f/SiOC composites have exhibited good mechanical properties and appeared as an interesting material for thermostructural applications [8,9].

Some applications (such as components for advanced space launch vehicles) concern high temperature utilization in space environment. However, these applications require exposure to reduced pressure environment. Therefore there is a strong need to understand their high temperature behavior at the temperature where the degradation of mechanical properties can take place in reduced pressure environment. The matrix functions to hold the fibers in place and to transfer the load to the fibers. The properties of the matrix are, never the less, very important in providing unique characteristics to the composite. At high temperatures SiOC glasses undergo a redistribution of Si–O bonds and Si–C bonds leading to the formation of SiC and SiO_2, in the same temperature range, carbothermal reductions may be active leading to the weight loss and to a subsequent deterioration of the mechanical properties [10–12]. Thus, C_f/SiOC composites is expected to exhibit various microstructures and mechanical properties after annealed at various temperature. However, few studies have been devoted to the research of high temperature behavior of C_f/SiOC composites in reduced pressure environment.

In this article, C_f/SiOC composites were fabricated through precursor impregnation and pyrolysis (PIP) process using siloxane resin as precursor. The microstructures and mechanical properties of C_f/SiOC composites before and after thermal exposures at various temperatures were examined, and the effects of matrix evolutions on the mechanical property degradation of C_f/SiOC composites were revealed.

---

[*] Corresponding author. Tel.: +86 731 84573169; fax: +86 731 84573165.
E-mail address: nudtmqs1975@163.com (T. Xu).

0272-8842/$36.00 © 2011 Elsevier Ltd and Techna Group S.r.l. All rights reserved.
doi:10.1016/j.ceramint.2011.07.049

2. Experimental procedure

2.1. Sample preparation

Commercially available polymethyl(phenyl)siloxane resin (Dow Corning 249 flake resin) was used as the precursor to SiOC glasses. Three-dimensional braided carbon fibers (T-300, ex-PAN carbon fiber, Toray) were used as the reinforcement for this study. The preparation of C_f/SiOC consisted on the following steps: (i) carbon fiber preforms were infiltrated with siloxane resin solution in vacuum, (ii) these performs filled with precursor were cured at 250 °C for 4 h in air and (iii) the cured preforms were pyrolyzed at 1000 °C with a heat rate of 20 °C/min under an inert atmosphere held for 1 h. The C_f/SiOC composites denoted as raw sample were prepared using thirteen infiltration-cure-pyrolysis cycles.

To reveal the high temperature evolution of SiOC glass matrixes, SiOC bulks were obtained through pyrolysis of siloxane resin. Siloxane resin was cross-linked at 250 °C in air for 4 h, ball milled and finally sieved to particle size <75 μm. Green bodies were obtained by cold pressing of powder at 130 MPa. SiOC bulks were obtained through pyrolysis of green bodies in flowing argon with a heat rate of 20 °C/min up to 1000 °C held for 1 h.

Those C_f/SiOC composites and SiOC bulks were further annealed at 1200, 1250, 1300, 1350, 1400, and 1500 °C in pressure of 10 Pa for 1 h at a heating rate of 15 °C/min to follow their evolutions.

2.2. Analytical methods

Three-point bending tests were used to evaluate the flexural strength and elastic modulus of C_f/SiOC composites with the span/height ratio of 15 and a cross-head motion speed of 0.5 mm/min. The number of test specimens was five. The bulk densities of the composites were measured according to Archimede's principle with deionized water as the immersion medium. Quantitative elemental analysis (EA) of the samples was performed on LECO CS600 for C and TCH600 for O. The perchloric acid dehydration gravimetric method was adopted for the determination of Si content. X-ray diffraction (Bruker D8 advance) with Cu K_α radiation was used to verify the crystal phases. Raman spectra were obtained using a Confocal laser Microraman Spectrometer (Jobin Yvon LABRAM-HR) with a 514.5 nm line of laser. Microstructures were analyzed by scanning electron microscopy (SEM; Hitachi S4800) and transmission electron microscopy (TEM; Tecnai F20). ^{29}Si MAS NMR spectra were measured with a Varian InfinityPlus 300 NMR spectrometer 59.56 MHz. The reference materials for chemical shift were tetramethysilane (TMS), and its chemical shift was adjusted to 0 ppm. Spinning rates of the samples at a magic angle was 4.0 kHz, and recycle time was 30 s.

Table 1
Effects of annealing temperature on the mechanical properties of C_f/SiOC composites.

Annealing temperature (°C)	Weight loss (wt.%)	Density (g/cm^3)	Flexural strength (MPa)	Elastic modulus (GPa)
–[a]	–	1.64 ± 0.02	330 ± 17	72 ± 6
1200	0.49	1.65 ± 0.02	358 ± 11	75 ± 9
1250	0.86	1.63 ± 0.03	344 ± 13	76 ± 5
1300	7.34	1.48 ± 0.02	193 ± 6	50 ± 4
1350	12.62	1.39 ± 0.03	90 ± 4	28 ± 3
1400	22.08	1.25 ± 0.04	28 ± 2	8 ± 1
1500	27.30	1.16 ± 0.03	19 ± 1	8 ± 1

[a] The raw sample.

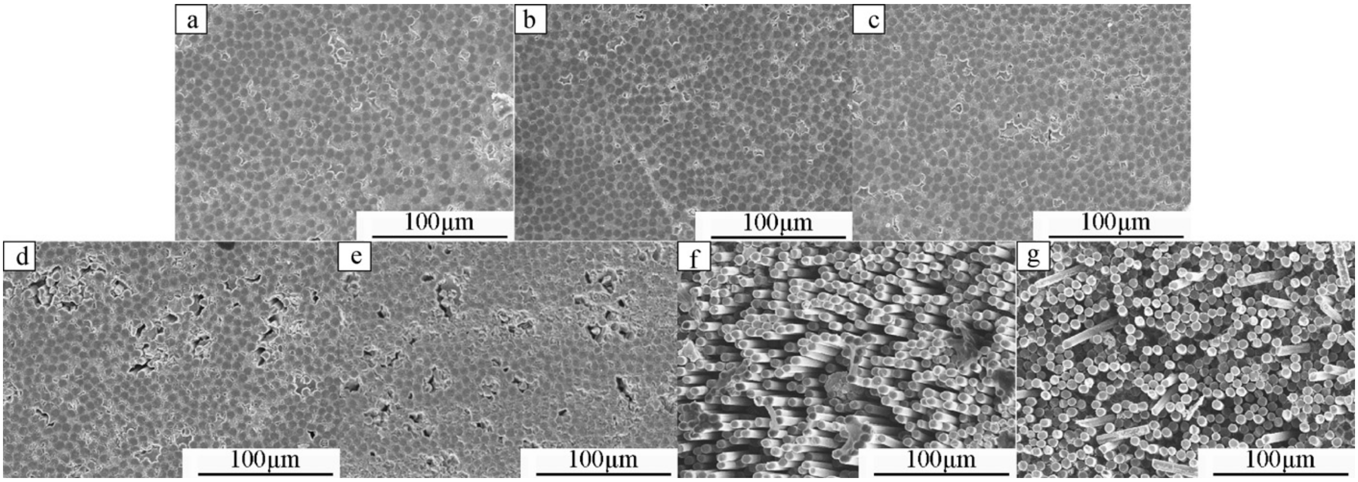

Fig. 1. SEM images of the cross sections of C_f/SiOC composites with various temperatures annealing: (a) the raw sample, (b) 1200 °C, (c) 1250 °C, (d) 1300 °C, (e) 1350 °C, (f) 1400 °C, (f) 1500 °C.

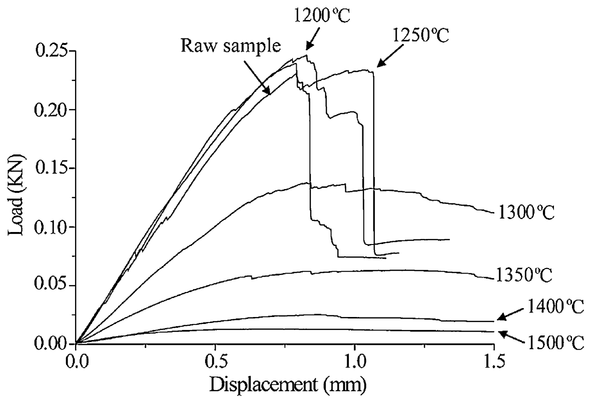

Fig. 2. Load–displacement curves of C_f/SiOC composites after annealed at various temperatures.

3. Results and discussion

3.1. Microstructure and mechanical property evolutions of C_f/SiOC composites

The mechanical properties of C_f/SiOC composites after annealed at various temperatures are reported in Table 1. It shows clearly that those heat-treated C_f/SiOC composites exhibit various mechanical properties. The mechanical properties and weight of C_f/SiOC composites are almost constant up to 1250 °C. Once the temperature is higher than 1300 °C, degradation of mechanical properties and weight loss are remarkable. Indeed, the flexural strength and elastic modulus of C_f/SiOC composites after 1500 °C annealing are only 6% and 11%, respectively, of that of the raw samples.

The SEM images of the cross sections of C_f/SiOC composites after annealed at various temperatures are shown in Fig. 1. On increasing the annealing temperature, the cross sections of C_f/SiOC composites undergo remarkable morphology changes. At temperature below 1250 °C, the fibers are surrounded by almost completely dense matrixes, and no evident changes can be observed. At temperature above 1300 °C, much small pores (about 1–10 μm) can be found in matrixes, and thus leading to the formation of loosen matrixes. Once the temperature reaches 1500 °C, a large amount of the space occupied by matrix in the raw samples becomes empty. It is resulted from the decomposition of SiOC matrix.

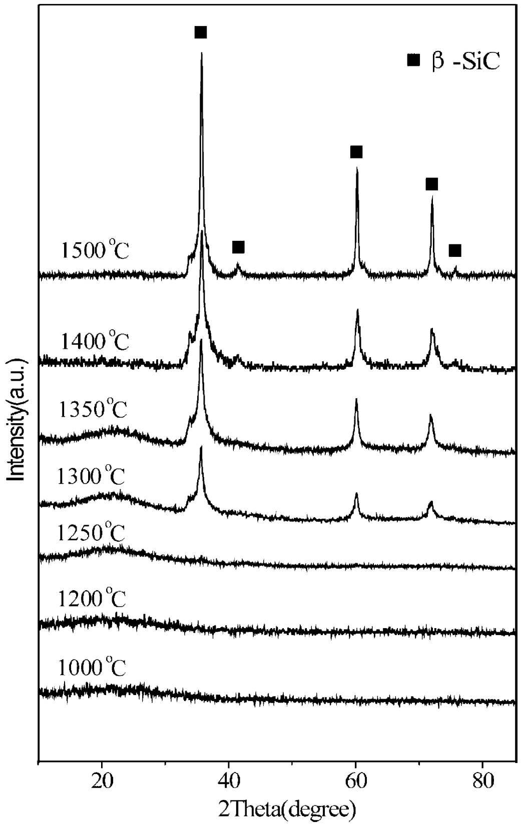

Fig. 3. XRD patterns of SiOC glasses after annealed at various temperatures.

It is well known that the matrix has a great effect on the mechanical properties of composites by holding the fibers in place and transferring the load to the fibers. Once the matrix decomposition occurs, induce the load cannot transfer to fibers, the degradation of mechanical properties of composites will be ineluctable. Fig. 2 is the load–displacement curves of C_f/SiOC composites after annealed at various temperatures. At temperature below 1250 °C, no significant changes can be observed. Once the temperature is above 1300 °C, the maximum force and slope of tangent to the initial straight-line decrease with the increasing temperatures. It is directly related that the load cannot effectively transferred to fibers caused by the decomposition of matrix. Therefore, in order to reveal the microstructure evolutions and mechanical property degradations of C_f/SiOC composites, a completely understanding about the high temperature behavior of SiOC glass matrix in reduced pressure environment is necessary.

Table 2
Elemental analysis and char yield measured on SiOC glasses after annealed at various temperatures.

Temperature (°C)	Linear shrinkage (%)	Yield (%)	Composition (wt%)			Oxycarbide stoichiometry
			Si	O	C	
1000	–	–	35.96	26.87	34.85	SiO1.31C0.34 + C1.91
1200	0.2	98.67	36.47	27.13	35.32	SiO1.30C0.35 + C1.91
1250	0.3	96.20	35.88	27.08	34.97	SiO1.32C0.33 + C1.93
1300	4.6	82.44	41.73	22.85	34.56	SiO0.96C0.52 + C1.41
1350	8.8	72.30	46.04	19.07	32.98	SiO0.72C0.64 + C1.03
1400	13.9	55.34	62.71	6.41	30.26	SiO0.18C0.91 + C0.22
1500	15.1	47.40	66.12	0.53	32.37	SiO0.01C0.99 + C0.15

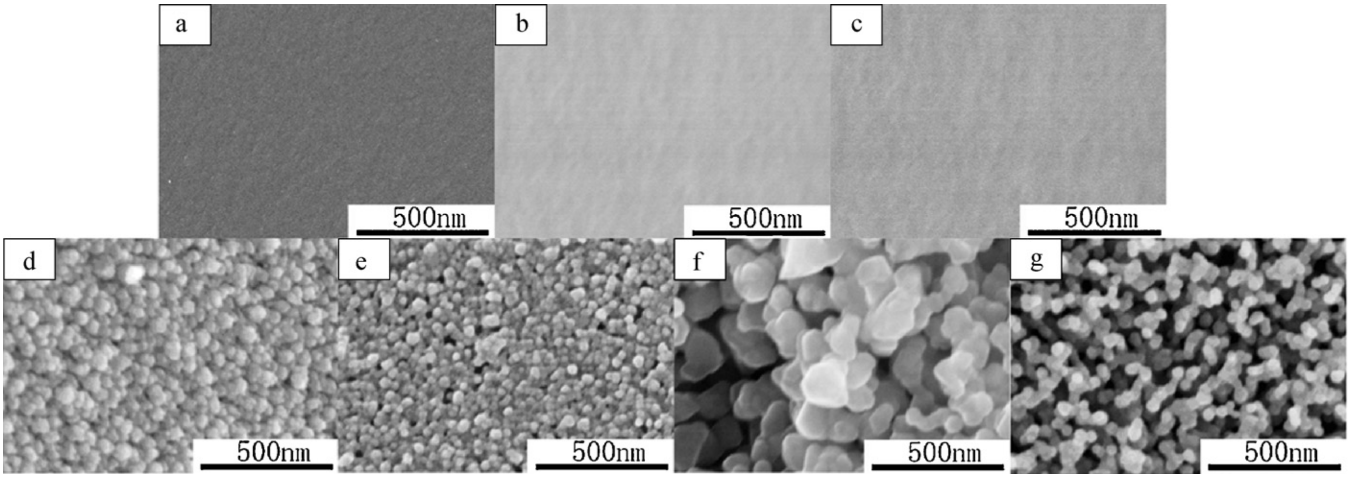

Fig. 4. SEM micrographs characteristic for SiOC glasses after annealed at various temperatures. (a) 1000 °C; (b) 1200 °C; (c) 1250 °C; (d) 1300 °C; (e) 1350 °C; (f) 1400 °C; (g) 1500 °C.

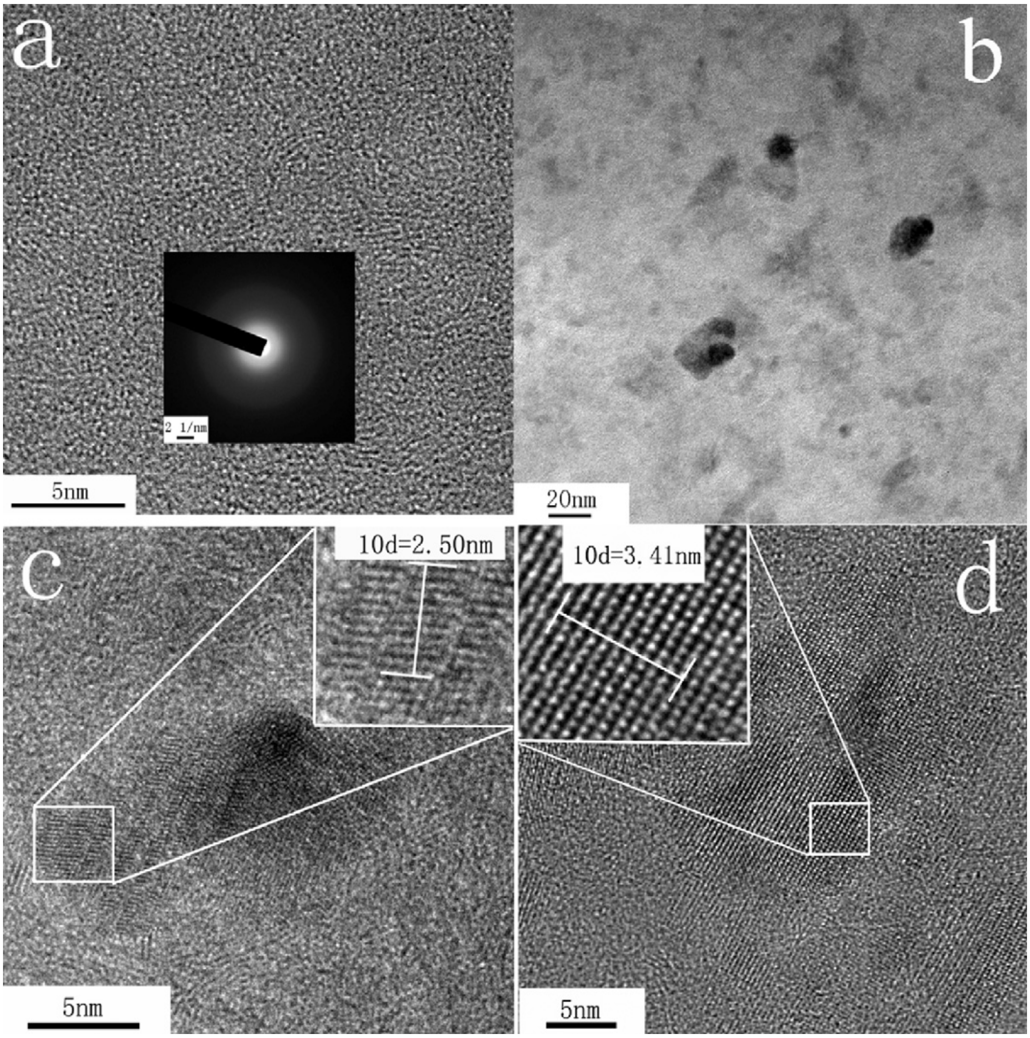

Fig. 5. TEM micrographs examined from SiOC glasses annealed at various temperatures. (a) HRTEM image of SiOC samples at 1000 °C with inset of the corresponding EDP. (b) Low magnification image characteristic for SiOC samples annealed at 1300 °C. (c), (d) HRTEM image of dark domains showed in (b), showing the presence of both SiC and graphite.

3.2. High temperature behavior of SiOC glasses in reduced pressure environment

The char yield and elemental analysis (EA.) results for SiOC glasses heat treated at various temperatures are reported in Table 2. It shows clearly that chemical compositions of samples are almost constant up to 1250 °C, despite the observation of a small weight loss (≈4%). From 1250 to 1500 °C, increasing ratio of Si/O and decreasing char yield can be observed. This behavior is directly related to carbothermal reductions occurring between SiO_2 and free carbon. The overall reaction usually proposed for carbothermal process can be described as Eq. (1).

$$SiO_2(s) + 3C(s) \rightarrow SiC(s) + 2CO(g) \quad (1)$$

This reaction is endothermic and should proceed in the following two steps [13]:

$$SiO_2(s) + C(s) \rightarrow SiO(g) + CO(g) \quad (2)$$

$$SiO(g) + 2C(s) \rightarrow SiC(s) + CO(g) \quad (3)$$

The temperature, at which the reaction (2) is initiated, is strongly dependent on pressure. It is governed by Eq. (4).

$$\Delta G = \Delta G^0 + \Delta nRT \ln\left(\frac{p}{p^0}\right) \quad (4)$$

where $\Delta G^0 = G_{SiO} + G_{CO} - G_{SiO2} - G_C$, $\Delta n = 2$, R = gas constant, T = temperature, p = pressure. According to Eq. (4), a higher pressure will shift the start of reaction (2) to higher temperatures. When $\Delta G = 0$ the temperature is 1110 °C in pressure of 10 Pa whereas the temperature will shift to about 1749 °C in pressure of 101 kPa. This suggests that a lower pressure will lead to a lower decomposition temperature of SiOC glasses [14].

XRD analysis was carried out to determine the crystalline phase. As shown in Fig. 3, those samples treated at temperature below 1250 °C are typical amorphous phases. The β-SiC phase and amorphous SiO_2 (broad halo centered at ~22°) is present at 1300 °C. Up to 1400 °C, only β-SiC phase can be observed. At temperature above 1400 °C, the strong, sharp peaks indicate a good crystalline β-SiC. Thus, β-SiC was confirmed as the main crystalline phase of the samples.

SEM micrographs examined from SiOC glasses annealed at various temperatures are reported in Fig. 4. Samples showed smooth fracture surfaces at lower temperature (<1250 °C). Once temperature is above 1300 °C, rough fracture surfaces composed of "particles" with diameters bellow 100 nm can be observed. These observations indicates that samples treated below 1250 °C are dense materials whereas samples treated above 1300 °C are porous materials. This evolution resulted from the weight loss and volume shrinkage during carbothermal process.

TEM was used to reveal the microstructure of SiOC glasses annealed at various temperatures (Fig. 5). The samples annealed 1000 °C are completely amorphous as shown in the HRTEM image and its associated electron diffraction patterns (EDP) (Fig. 5a). Fig. 5b shows the low-magnification image of sample annealed at 1300 °C. The dark domains with diameter of 20–30 nm can clearly be seen. They are assumed to crystalline phase embedded in dense amorphous matrix. Those dark domains were further identified as shown in Fig. 5c and d. The lattice fringes can be seen, with 0.25 nm of (1 1 1) plane spacing of the β-SiC crystal and 0.33 nm of (0 0 2) plane spacing of the graphite.

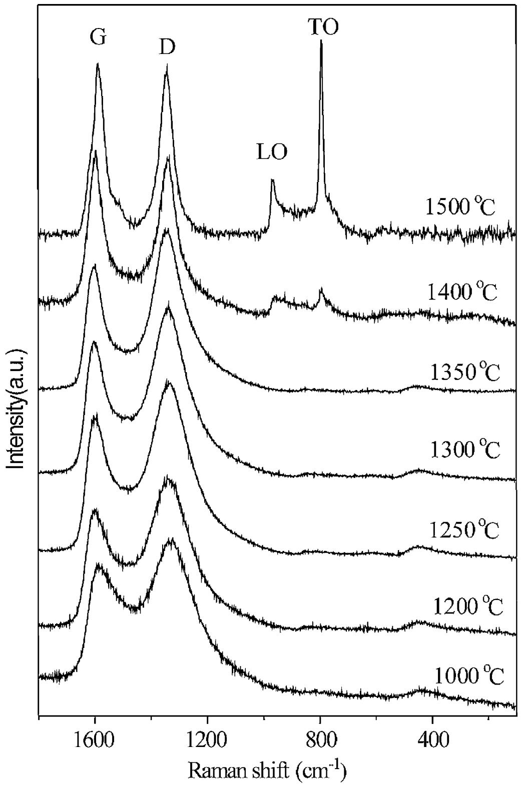

Fig. 6. Raman spectra of SiOC glasses after annealed at various temperatures.

Raman spectra of SiOC samples annealed at various temperatures are reported in Fig. 6. Significant changes for spectral parameters such as peak position, half-width and the integrated intensity of different bands can be observed from 1000 to 1500 °C. In order to determine those spectral parameters, band separation was performed employing Gauss–Lorentz function. The spectra were separated to the three bands at around 1335, 1535 and 1600 cm^{-1}. The bands centered at around 1600 and 1335 cm^{-1} are related to the G band and D band [15] and the band centered at around 1535 cm^{-1} reflects the presence of interstitial disorder site within the sample [16].

The peak position, half-width and the ratio (I_D/I_G) of D and G bands are reported in Table 3. On increasing the annealing temperature, the increase in the intensity of G band and decrease of its half-width can be observed. It is directly related to the increasing orientation of the carbon structure [17]. The ratio (I_D/I_G) is related to in-plane crystallite size, La, of graphite domains. The crystallite size was calculated by using the following relation: La = 4.4 $(I_D/I_G)^{-1}$[15]. It shows that the size of graphite crystallite increases with the increase of temperature.

In addition, two peaks at around 792 cm^{-1} and 966 cm^{-1} can be observed at temperature above 1400 °C. The two signals were assigned to the mode of transverse optical (TO) and longitudinal optical (LO) phonon, respectively, at the Γ point of the cubic SiC (known as β-SiC) [18]. It is worth noting that β-SiC has formed at 1300 °C as reported by XRD. However, no

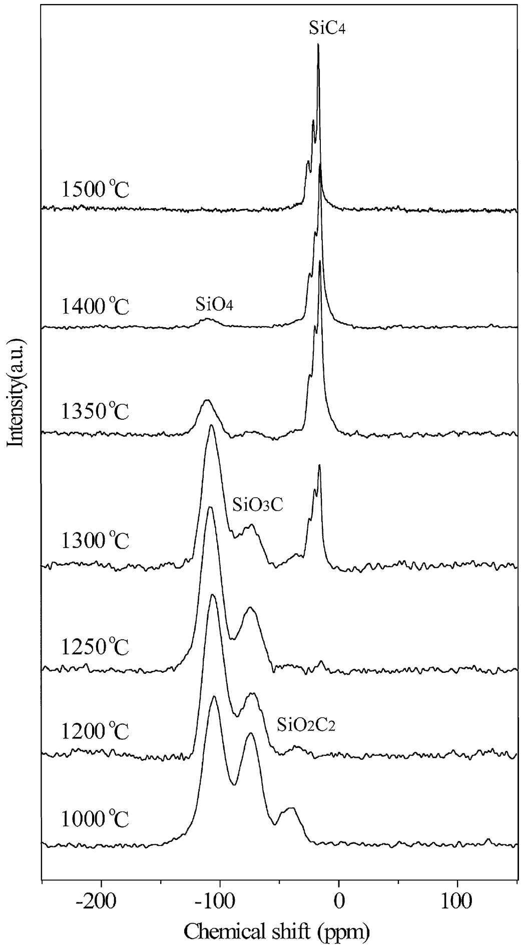

Fig. 7. ^{29}SiMAS NMR spectra of SiOC glasses annealed at various temperatures.

Table 3
Raman characteristics of the free carbon in SiOC glasses after annealed at various temperatures.

Temperature (°C)	Band (cm^{-1})	Width (cm^{-1})	Ratio (I_D/I_G)	Size (Å, C = 44)
1000	1328	193	2.6	17
	1534	150		
	1587	82		
1200	1334	178	2.1	21
	1544	144		
	1599	80		
1250	1332	166	1.9	26
	1545	140		
	1601	69		
1300	1336	157	1.7	26
	1550	132		
	1605	66		
1350	1340	81	1.4	29
	1536	127		
	1599	60		
1400	1341	82	1.1	40
	1523	124		
	1598	60		
1500	1325	59	1.1	40
	1537	121		
	1587	52		

Raman signals of β-SiC can be observed at 1300 °C. It is related to the relative low Raman efficiency of SiC.

The ^{29}Si MAS NMR spectra obtained from samples after annealed at various temperatures are reported in Fig. 7. Depending on the annealing temperature, SiOC exhibits various amounts of the SiO_xC_{4-x} tetrahedral sites ($SiO_4 \sim -108$ ppm, $SiCO_3 \sim -74$ ppm, $SiC_2O_2 \sim -34$ ppm, $SiC_4 \sim -16$ ppm) [19]. At 1000 °C, the sample consists primarily of SiO_4, SiO_3C, and SiO_2C_2, with a smaller amount of, or without, $SiOC_3$ and SiC_4 units. On increasing the annealing temperature, the NMR data show a redistribution of bonds within the system. The evolution is gradually staring from 1000 °C to 1400 °C as shown in Eq. (5).

$$SiO_xC_{4-x} \rightarrow \frac{x}{4}SiO_4 + \frac{4-x}{4}SiC_4 \tag{5}$$

Additionally, at temperature above 1300 °C, a peak emerges at around −16 ppm is assigned to SiC_4 units. It is even possible to distinguish several peaks at −16, −20, and −25 ppm, which are due to the presence of crystalline β-SiC, with some α-SiC [20].

The compositions of the silicon oxycarbide network detected by ^{29}Si MAS NMR experiments are reported in Table 4. The oxygen content within silicon oxycarbide network seems overestimated in the NMR spectra compared with the EA results. However, comparison between samples can be made to extract general trend: (i) bonds redistribution occurred at temperature from 1000 to 1250 °C, leading to the increasing content of SiO_4 unite. (ii) Carbonthermal reductions are active at temperature

Table 4
Quantitative analysis determined for Si species.

Temperature (°C)	Si species (%)				SiOC composition	
	SiO_4	SiO_3C	SiO_2C_2	SiC_4	From NMR	From EA
1000	54	35	11	NA	SiO1.72C0.14	SiO1.31C0.34
1200	66	28	6	NA	SiO1.80C0.10	SiO1.30C0.35
1250	64	30	4	2	SiO1.77C0.11	SiO1.32C0.33
1300	54	22	5	19	SiO1.46C0.27	SiO0.96C0.52
1350	33	7	NA	60	SiO0.77C0.62	SiO0.72C0.64
1400	15	NA	NA	85	SiO0.30C0.85	SiO0.18C0.91
1500	NA	NA	NA	100	SiO0.00C1.00	SiO0.01C0.99

NA: Cannot be detected by NMR.

from 1300 to 1500 °C, leading to the decreasing content of SiO_4 unite. It accord with the results of EA discussed above.

From the results discussed above, it can be found that the temperature plays a crucial role on microstructure and composition of SiOC glasses. On increasing the temperature Raman data show an increasing orientation of crystalline carbon in SiOC glasses. Carbothermal reductions are active at 1300 °C and almost complete at 1500 °C. Due to the weight loss during carbothermal process, SiOC glasses treated at above 1300 °C are porous materials whereas samples treated at bellow 1250 °C are dense materials. Bonds redistribution occurs at above 1000 °C, and almost finished at 1400 °C.

4. Conclusion

C_f/SiOC composites were prepared by the precursor impregnation and pyrolysis process, and then those composites were annealed at various temperatures to follow their microstructure and mechanical property evolutions. It was found that the annealing temperature played a crucial role on the microstructure and mechanical properties of C_f/SiOC composites. At temperature below 1250 °C, the mechanical properties of C_f/SiOC composites are almost constant. In this temperature range, the volume and weight of SiOC matrixes do not change too much, despite the matrixes undergo a redistribution of Si–O bonds and Si–C bonds leading to the formation of SiC and SiO_2. At temperature above 1300 °C, both the flexural strength and elastic modulus of C_f/SiOC composites decrease rapidly with increasing temperature. This behavior is directly related to the decomposition of matrixes. In this decomposition process, the weight loss and volume shrinkage of SiOC matrixes are remarkable, and thus the load cannot be effectively transferred to fibers.

Acknowledgements

This study was supported by Hunan Provincial Natural Science Foundation of China (no. S2010J504B), National Defense Preliminary Research Program of China (no. 9140C8203040904), and Natural Science Foundation of China (no. 90916002).

References

[1] C. Pantano, A. Singh, H. Zhang, Silicon oxycarbide glasses, J. Sol-Gel Sci. Technol. 14 (1999) 7–25.

[2] S. Walter, G.D. Soraru, H. Brequel, S. Enzo, Microstructural and mechanical characterization of sol gel-derived Si–O–C galsses, J. Eur. Ceram. Soc. 22 (2002) 2389–2400.

[3] Y.D. Blum, D.B. MacQueen, H.-J. Kleebe, Synthesis and characterization of carbon-enriched silicon oxycarbides, J. Eur. Ceram. Soc. 25 (2005) 143–149.

[4] G.D. Soraru, S. Modena, E. Guadagnino, P. Colombo, J. Egan, C. Panatano, Chemical durability of silicon oxycarbide glasses, J. Am. Cream. Soc. 85 (2002) 1529–1536.

[5] H.J. Yu, X.G. Zhou, W. Zhang, H.X. Peng, C.R. Zhang, Z.L. Huang, Mechanical properties of 3D KD-I SiC_f/SiC composites with engineered fibre-matrix interfaces, Compos. Sci. Technol. 71 (2011) 699–704.

[6] Y. Yu, J. Tai, X. Tang, Y. Guo, M. Tang, X. Li, Continuous Si–C–O–Al fiber derived from aluminum-containing polycarbosilane precursor, Compos. Part A 39 (2008) 1101–1105.

[7] A. Delcamp, L. Maille, S.S. Martin, R. Pailler, A. Guette, Al–O–N. and Al–O–B–N thin films applied on Si–O–C fibers, Compos. Sci. Technol. 70 (2010) 622–626.

[8] P.N. Adler, Overview of arpa low-cost ceramic composites (LC3) program, in: 41st International SAMPE Symposium, March 24–28, (1996), pp. 524–531.

[9] Q.S. Ma, Z.H. Chen, W.W. Zhen, H.F. Hu, Effects of pyrolysis processes on microstructure and mechanical properties of Cf/Si–O–C composites fabricated by preceramic polymer pyrolysis, Ceram. Int. 31 (2005) 305–314.

[10] L. Bois, J. Maquet, F. Babonneau, Structural characterization of sol–gel derived oxycarbide galsses. 2. Study of the thermal stability of the silicon oxycarbide phase, Chem. Mater. 7 (1995) 975–981.

[11] G.D. Soraru, D. Suttor, High temperature stability of sol–gel-derived SiOC glasses, J. Sol-Gel Sci. Technol. 14 (1999) 69–74.

[12] J. Parmentier, G.D. Soraru, F. Babonneau, Influence of the microstructure on the high temperature behavior of gel-derived glasses, J. Eur. Ceram. Soc. 21 (2001) 817–824.

[13] H.P. Martin, R. Ecke, E. Muller, Synthesis of nanocrystalline silicon carbide powder by carbothermal reduction, J. Eur. Ceram. Soc. 18 (1998) 1737–1742.

[14] T. Xu, Q. Ma, Z. Chen, The effect of environment pressure on high temperature stability of silicon oxycarbide glasses derived from polysiloxane, Mater. Lett. 65 (2011) 1538–1541.

[15] F. Tuinstra, J.L. Koenig, Raman spectrum of graphite, J. Chem. Phys. 53 (1970) 1126–1130.

[16] T. Jawahari, A. Road, J. Casado, Raman spectroscopic characterization of some commercially available carbon black materials, Carbon 33 (1995) 1561–1565.

[17] S. Karlin, Ph. Colomban, Raman study of the chemical and thermal degradation of as-received and sol–gel embedded Nicalon and Hi-Nicalon SiC fibers used in ceramic matrix composites, J. Raman Spectrosc. 28 (1997) 219–228.

[18] M. Bechelany, A. Brioude, D. Cornu, G. Ferro, P. Miele, A raman spectroscopy study of individual SiC nanowires, Adv. Funct. Mater. 17 (2007) 939–943.

[19] H. Brequel, J. Parmentier, S. Walter, R. Badheka, G. Trimmel, S. Masse, J. Latournerie, P. Dempsey, C. Turquat, A. Desmartin-Chomel, L. Le Neindre-Prum, U.A. Jayasooriya, D. Hourlier, H.-J. Kleebe, G.D. Soraru, S. Enzo, F. Babonneau, Systematic structural characterization of the high-temperature behavior of nearly stoichiometric silicon oxycarbide glasses, Chem. Mater. 16 (2004) 2585–2598.

[20] D.C. Apperley, R.K. Harris, G.L. Marshall, D.P. Thompson, Nuclear magnetic resonance studies of silicon carbide polytype, J. Am. Ceram. Soc. 74 (1991) 777–782.